



Ionic liquids as solvents for Čerenkov counting and the effect of a wavelength shifter

M. Mirenda^{a,*}, D. Rodrigues^a, C. Ferreyra^b, P. Arenillas^b, G.P. Sarmiento^c, N. Krimer^c, M.L. Japas^c

^a Comisión Nacional de Energía Atómica (CNEA), CONICET, Gerencia Química, Centro Atómico Constituyentes, Av. Gral. Paz 1499, San Martín, B1650KNA Buenos Aires, Argentina

^b Comisión Nacional Energía Atómica (CNEA), Unidad de Actividad Radioquímica, Centro Atómico Ezeiza, Pro González y Aragón 15, Ezeiza, B1802AYA Buenos Aires, Argentina

^c Comisión Nacional de Energía Atómica (CNEA), Gerencia Química, Centro Atómico Constituyentes, Av. Gral. Paz 1499, San Martín, B1650KNA Buenos Aires, Argentina

HIGHLIGHTS

- Wavelength shifter effect with a highly fluorescent ionic liquid on the Čerenkov radiation was studied.
- Activities of high energy β emitters can be quantified by TDCR-Čerenkov technique using fluorescent ILs mixture.
- A significant increment in a TDCR detection efficiency was achieved using a fluorescent ionic liquid mixture.
- The addition of a wavelength-shifter breaks the anisotropy of the Čerenkov radiation.

ABSTRACT

We study the wavelength shift of the Čerenkov light – generated in the ionic liquid (BMIMCl) – caused by the addition of the highly fluorescent ionic liquid (BMIMHPTS). ^{18}F and ^{32}P efficiencies increases up to 124% and 14%, respectively, compared with the values obtained with pure BMIMCl. With this improvement, ionic liquid mixtures become a good alternative – when using the TDCR-Cherenkov technique – to standardize radionuclides having electron emissions energies close to the threshold energy in water (~ 260 keV). As an advantage compared with other solvents, the ionic liquid mixture can be reused, in the case of short-lived radionuclides, by simply removing all water content in a vacuum oven.

1. Introduction

Ionic liquids (ILs) are organic salts with melting points near room temperature, with 100 °C as agreed arbitrary upper limit (Weingärtner, 2008). The ionic nature of these liquids gives them distinctive physicochemical properties compared with traditional organic solvents, mostly toxic, volatile and flammable, while the chemical characteristics of either cation and/or anion give ILs a tunable solvation power (Welton, 1999; Isik et al., 2014). The moderate thermal stability, low flammability, and good conductivity are some of the remarkable features that justify their nascent application, e.g. in nuclear technology (Sun et al., 2012). In particular, we have previously reported the use of the common IL 1-butyl-3-methylimidazolium chloride (BMIMCl) to standardize the activity of an ^{18}F solution (emitting positrons up to 634 keV) by means of the Čerenkov counting technique (Mirenda et al., 2014).

The intensity of Čerenkov radiation depends on the refractive index n of the medium (Tamm, 1939). The higher n , the lower the Čerenkov energy threshold and hence the higher the probability for Čerenkov light emission. In this sense, the relatively high refractive index of BMIMCl makes it very convenient for this kind of measurement (Mirenda et al., 2014). Furthermore, there is another important issue to attend in order to increase the detection efficiency, which is the matching between the emission spectra and the photocathode sensitivity. Thus, the addition of a suitable dye can shift the emission wavelength range of the primary component of the cocktail to a wavelength range more compatible with the region of high photocathode sensitivity.

Here, we propose the use of a novel fluorescent IL, the 1-butyl-3-methylimidazolium 8-hydroxypyrene-1,3,6-trisulfonate (BMIMHPTS), to act as a wavelength shifter of the Čerenkov photons generated from BMIMCl. The work comprises two main parts: Section 2 describes the

* Corresponding author.

E-mail address: mirenda@cnea.gov.ar (M. Mirenda).

synthesis and the optical characterization of BMIMHPTS/BMIMCl mixtures and, Section 3 presents the results of nuclear measurements. In Section 2 we show that the absorption and emission spectra of BMIMHPTS match very well with the Čerenkov spectrum and the region of maximum photomultiplier tube efficiency, respectively. In order to experimentally confirm the wavelength shifting of the Čerenkov light, in Section 3 we document the luminescent spectra emerging from a quartz cell with BMIMCl and a β emitter radionuclide, with and without the addition of BMIMHPTS. The TDCR-Čerenkov method was used to calculate the counting efficiency for the logical sum of double coincidences, ϵ_D . Experiments with increasing amounts of wavelength shifter allowed us to find the optimal BMIMHPTS concentration that maximizes the counting efficiency ϵ_D . Finally, the wavelength shift effect on the anisotropic nature of the Čerenkov radiation was also studied. Conclusions and perspectives are given in Section 4.

2. Synthesis and optical measurements

2.1. Reagents and samples preparation

BMIMCl was synthesized and purified as described in a previous work (Sarmiento et al., 2016). BMIMHPTS was synthesized from BMIMCl and pyranine (8-hydroxypyrene-1,3,6-trisulfonic acid trisodium salt, Aldrich, purity > 97%) via a metathesis reaction. The chemical structure of BMIMHPTS, supported by ^1H NMR (proton Nuclear Magnetic Resonance spectroscopy) measurement (data not shown), is given in Fig. 1.

BMIMCl / BMIMHPTS mixtures were prepared by addition of weighted amounts of both ILs. The density of all solutions was 1.07 g/mL. The samples were heated at 60 °C in a water bath, and mixed during a day with magnetic stirring to ensure the complete homogenization. Afterwards, mixtures were cooled to room temperature. All measurements were performed at the thermostatic condition of 20 °C.

The refractive indices of the IL mixtures were measured at 589.3 nm in a thermostated Abbemat 300™ automatic refractometer (Anton Paar). The values obtained for BMIMCl with and without BMIMHPTS are $n = 1.509(1)$.

2.2. Absorption and steady-state fluorescence

Absorption spectra were acquired in a Cary 50 Conc UV-Vis Spectrophotometer (Varian), equipped with a thermostated sample-holder. Steady-state fluorescence spectra were recorded with a commercial PTI QuantaMaster™ 4 CW fluorometer, equipped with a xenon short-arc lamp UXL-75XE and a thermostated sample-holder. The fluorescence spectra of the samples were measured in a transmission configuration (180°) ensuring small excitation and detection volumes, in order to avoid that the re-emitted radiation reaches the detector. In this configuration, only re-absorption is present (Krimmer et al., 2016). Quartz cells (Spectrosil™) of 2 mm optical path-length were used for the optical measurements.

The fluorescence quantum yield (Φ_F) was determined using a

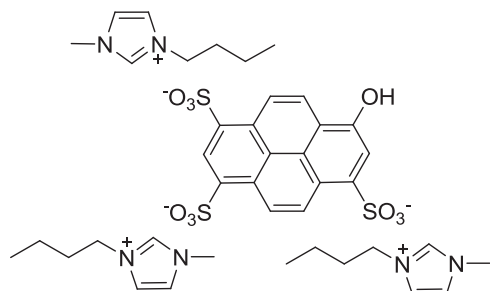


Fig. 1. Chemical structure of 1-butyl-3-methylimidazolium 8-hydroxypyrene-1,3,6-trisulfonate ionic liquid.

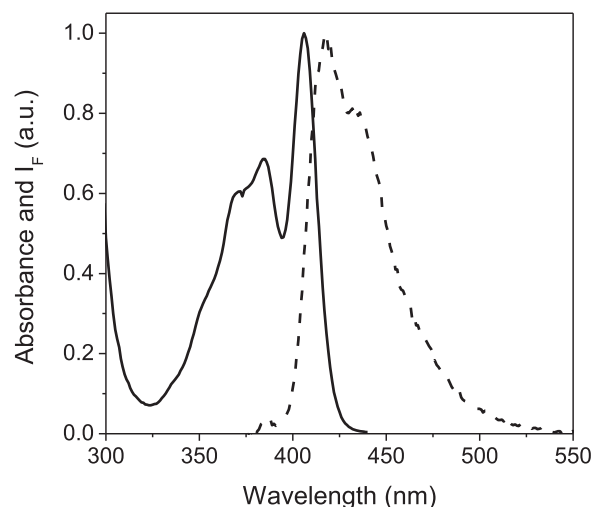


Fig. 2. Normalized absorption (solid line) and fluorescence (dashed line) spectra of a 2.7×10^{-5} M solution of BMIMHPTS in BMIMCl. Optical path-length = 2 mm.

diluted BMIMHPTS solution (2.7×10^{-5} M) in BMIMCl. Only in this case, the fluorescence measurements were carried out in a 90° configuration with a quartz cell of 10 mm optical path-length. An acidic aqueous solution of quinine bisulfate (8.3×10^{-5} M, in 0.5 M of H_2SO_4) was used as reference ($n = 1.3384$, $\Phi_F = (\text{QBS}) = 0.546$; Dawson and Windsor, 1968).

Fig. 2 shows the normalized absorption and emission spectra of a 2.7×10^{-5} M solution of BMIMHPTS in BMIMCl. The photophysics of BMIMHPTS shows several advantageous features: a) the absorption spectrum is in the range of the emitted Čerenkov photons, b) the emission spectrum has a maximum at 418 nm, which matches very well with the maximum responsivity of the Quantacom™ Burle 8850 photomultipliers (375–450 nm) used in our TDCR (Triple to Double Coincidence Ratio) system, and c) it has a very high $\Phi_F = 0.98(2)$.

A remarkable feature is that, in aqueous environment, the HPTS anions show two different absorption and emission spectra corresponding to the presence of two acid-base species (Förster, 1950). However, the anion shows only the absorption and the emission spectra corresponding to the acidic species in BMIMCl, as this solvent is an extremely weak proton acceptor.

Two competing effects take place when the concentration of a fluorophore (like BMIMHPTS) is increased in solution: a) at low concentrations, the emission increases, as there are more emitting species, and b) at moderate or high concentrations, the emission decreases, due to re-absorption and to the presence of non-radiative events such as aggregation, self-quenching, etc. Then, there should be an optimal concentration of BMIMHPTS in BMIMCl, i.e. a concentration that maximizes the detection efficiency. In order to find the optimal concentration by means of optical measurements, we recorded the steady-state fluorescence emission spectra of different mixtures of BMIMHPTS in BMIMCl. As depicted in Fig. 3, between 5.9×10^{-6} M and 1.1×10^{-3} M, the fluorescence intensity I_F increases with concentration. For concentrations higher than 1.1×10^{-3} M the intensity of the emission diminishes, probably as a consequence of a self-quenching phenomenon. Furthermore, for concentration values higher than 1.3×10^{-4} M, the shape of the fluorescence spectra changes at the blue edge, as a consequence of re-absorption. The inset of the same figure shows that the total integrated intensity reaches a maximum at a concentration value of 1.1×10^{-3} M.

The optimal concentration value obtained from these experiments constitutes a first-order approximation, since the geometry of vials and the detector configuration in scintillation experiments may differ appreciably. Besides, it must be considered that the excitation light beam has a defined direction in these experiments, producing an exponential

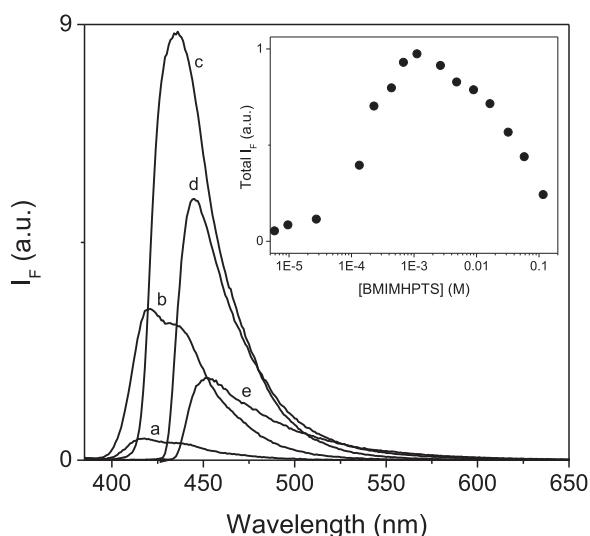


Fig. 3. Emission spectra of BMIMHPTS in BMIMCl for some selected concentrations: a) 5.9×10^{-6} M, b) 1.3×10^{-4} M, c) 1.1×10^{-3} M, d) 0.032 M and e) 0.032 M and f) 0.11 M. Inset: total emitted intensity as a function of BMIMHPTS concentration.

population of excited states along the path-length, whereas in a radioactive solution, the population of excited molecules presents a homogeneous distribution inside the cell. However, the photophysical study allows a drastic reduction of the concentration interval to be tested in scintillation experiments.

3. Nuclear measurements

3.1. Čerenkov shifted and non-shifted luminescence

A home-made optical arrangement was built to determine the effect produced by BMIMHPTS on the Čerenkov photons originated from BMIMCl. The experimental setup consists of a metallic cell-holder equipped with a filter-holder and a Hamamatsu™ R938-14 photomultiplier tube, which has an extended detection region (quantum efficiency above 5%) from 190 nm to 700 nm. The pure-beta emitter ^{32}P (half-life of 14.3 days and maximum electron energy of 1.73 MeV (Bé et al., 2004)) was chosen for the experiment. A 10 μL drop of the ^{32}P -aqueous solution (activity of ~ 500 kBq) was placed into each of two quartz cells of 10 mm \times 10 mm \times 30 mm size, containing BMIMCl and a BMIMCl/BMIMHPTS mixture, respectively. Six different Schott™ cut-off glass filters (WG295, WG345, WG395, GG435, GG475 and OG530) were intercalated, one at a time, between the sample-holder and the photomultiplier. Thereby, the covered spectral range was split into seven intervals.

The number of events as a function of pulse height (*i.e.* pulse height spectrum) was recorded for each interposed cut-off filter. The number of photons corresponding to each interval, Y_m , was calculated as the difference between the total events (weighted by pulse height) in two consecutive spectra. The cut-off wavelength of each filter was taken as the wavelength corresponding to the mean of minimum and maximum transmittance values. The main contribution to the Y_m uncertainties arises from the cut-off filter wavelength assessment. Uncertainties of 5 nm in the cut-off wavelengths of the filters were assigned by considering the wavelength interval around the mean value for which transmittance changes by 68%. Propagating these uncertainties gives an uncertainty of $\sim 17\%$ on Y_m . Adding this component in quadrature to the statistical uncertainties estimated from the number of events for each bin leads to a conservative estimate for the total combined relative uncertainty on Y_m of $\sim 20\%$.

Fig. 4 shows the Čerenkov emission of ^{32}P in BMIMCl, which has a maximum between 350 nm and 400 nm. The spectrum diminishes at

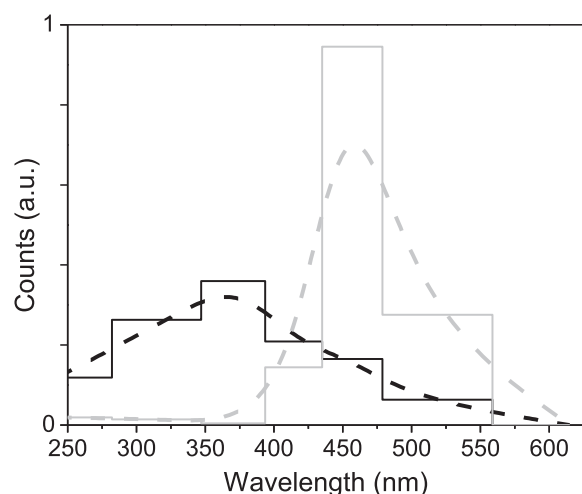


Fig. 4. Emission spectra from ^{32}P in BMIMCl with (gray line) and without BMIMHPTS (black line). The dashed lines represent B-spline smoothing.

the blue edge due to the re-absorption caused by the BMIMCl, which absorbs all photons with $\lambda < 250$ nm. Fig. 4 also shows that the addition of BMIMHPTS to BMIMCl: a) reduces the photons emitted between 250 nm and 400 nm and, b) increases the emission between 425 nm and 550 nm due to the fluorescence of the HPTS anions.

The reduction of the Čerenkov light at shorter wavelengths and the presence of fluorescence at higher wavelengths indicate the occurrence of energy transfer events. The low concentration of BMIMHPTS ($\sim 2.6 \times 10^{-4}$ M) points out the radiative nature of this phenomenon. At this concentration condition, the HPTS anions are separated by *ca.* 100 Å (Turro, 1991), a distance too large to allow non-radiative energy transfer processes.

The shifting of the emission spectrum toward higher wavelengths improves its overlap with the spectral photocathode sensitivity of Quantacom™ Burle 8850 photomultipliers. In fact, the integrated spectrum $S(\lambda)$ (normalized to unit area) weighted by the photomultiplier responsivity $R(\lambda)$, *i.e.*: $\int_{190\text{nm}}^{700\text{nm}} R(\lambda)S(\lambda)d\lambda$ results 15% higher when BMIMHPTS is present.

3.2. TDCR-Čerenkov method

The detection probability of at least one photon at the *i*th photo-detector can be calculated as:

$$P_i = 1 - e^{-\mu_i} \quad (1)$$

where μ_i is the number of photons arriving to the photocathode. In classical TDCR method $\mu_i = m(E) \cdot \nu$, where $m(E)$ is the mean number of photons produced by the scintillator (calculated from Birks's formula) and ν is a free parameter. In the case of electron produced Čerenkov radiation $\mu_i = k(E) \cdot \nu \cdot \alpha_i$, where $k(E)$ is the mean number of photons emerging from the medium and α_i is an anisotropic factor.

$k(E)$ can be calculated by combining the Frank and Tamm theory (Frank and Tamm, 1937) and the electrons stopping power from ESTAR database (ESTAR, 2009) as proposed by Kossert (2010):

$$k(E) \propto \int_{E_{th}}^E \frac{dk}{dx} \frac{1}{\rho} \frac{1}{dE'/dX} dE' \quad (2)$$

In Eq. (2), ρ is the density, dE/dX are the electron stopping powers, and $\frac{dk}{dx} \propto 1 - \frac{1}{n^2\beta^2}$, where n is the refractive index and β is the particle's velocity relative to the speed of light in the vacuum. The integration limit E_{th} corresponds to the threshold energy for Čerenkov radiation (Tamm, 1939), expressed as:

$$E_{th} = E_0 \left(\frac{1}{\sqrt{1 - n^{-2}}} - 1 \right) \quad (3)$$

where E_0 is the electron rest energy (0.511 MeV).

According to Kossert (2010), the α_i parameters –used to describe the anisotropic nature of Čerenkov radiation– are related in TDCR systems one to each other as:

$$\alpha_1 = \alpha, \quad \alpha_2 = 3/2(1 - \alpha) \alpha, \quad \alpha_3 = 1 - 3/2(1 - \alpha) \alpha - \alpha.$$

Hence, only one parameter α is necessary to describe the anisotropy. It is worth noting that, for the isotropic case, $\alpha = 1/3$. For the anisotropic case, $\alpha = 0.42$ was employed with excellent results (Kossert, 2010).

In the experimental TDCR-Čerenkov measurements, the free parameter ν is adjusted in order to recover the experimental triple to double ratio, T/D, which is expressed in Eq. (4).

$$\frac{T}{D} = \frac{\int_0^E N(E') \cdot (1 - e^{-\nu \cdot \alpha_1 \cdot k(E')}) \cdot (1 - e^{-\nu \cdot \alpha_2 \cdot k(E')}) \cdot (1 - e^{-\nu \cdot \alpha_3 \cdot k(E')}) dE'}{\int_0^E N(E') \cdot \left\{ \left[\frac{1}{2} \sum_{i=1}^3 \sum_{j=1}^3 (1 - \delta_{ij}) \cdot (1 - e^{-\nu \cdot \alpha_i \cdot k(E')}) \cdot (1 - e^{-\nu \cdot \alpha_j \cdot k(E')}) \right] - 2 \cdot (1 - e^{-\nu \cdot \alpha_1 \cdot k(E')}) \cdot (1 - e^{-\nu \cdot \alpha_2 \cdot k(E')}) \cdot (1 - e^{-\nu \cdot \alpha_3 \cdot k(E')}) \right\} dE'} \quad (4)$$

where $N(E)$ is the normalized energy beta spectrum and $k(E)$ is calculated from Eq. (2). Finally, ε_D values can be obtained from the denominator in the last expression.

In a recent work, Kossert et al. (2014) have included some improvements in these calculations, by considering: i) the wavelength dependence of the refractive index of the solvent, ii) the wavelength dependence of the photomultiplier response and, iii) potential PMT efficiency asymmetries. As a result, the relative error between experimental and theoretical efficiencies, for example in ^{32}P , is reduced from 0.64% to 0.27% (for $\alpha = 0.42$), representing a valuable contribution for standardization. However, since our work aims at studying the wavelength shifter effect in ILs mixtures, the accuracy that is mandatory for standardization measurements is not entirely required in this work. The precision reached by applying the Kossert (2010) methodology is sufficient to show and characterize the phenomena under study.

3.3. TDCR-Čerenkov results

The TDCR system at the Laboratorio de Metrología de Radioisótopos (LMR) from the Comisión Nacional de Energía Atómica Nacional (CNEA, Arenillas and Cassette, 2006) was used to obtain ε_D values and, thereby, to determine the optimal concentration of BMIMHPTS. Two drops of $\sim 10 \mu\text{L}$ aqueous solutions of ^{18}F and ^{32}P were introduced, respectively, in two sets of 20 mL glass vials containing 10 mL of BMIMCl. The activity of each sample was roughly estimated as $\sim 4 \text{ kBq}$, calculated from a dilution of an initial radioactive solution measured in a Capintec CRC-15R Activimeter. Next, different aliquots from a stock solution (concentration 0.15 M of BMIMHPTS in BMIMCl) were progressively dropped into the vials to increase the concentration of wavelength shifter. An extra sample of pure BMIMCl without activity was used as background.

Table 1 summarizes the results obtained in TDCR-Čerenkov experiments. The experimental ε_D values were calculated from the double coincidence counting obtained in the TDCR-Čerenkov method relative to those obtained from the TDCR LSC method with Ultima Gold AB™. In this way, ^{18}F electron capture probability is not included in the calculations. The potential gamma interaction inside the photocathodes via Compton effect was not taking into account in this approach. The uncertainties in Table 1 are mainly determined by the statistical uncertainties in the coincidence counting (in both TDCR-Čerenkov and TDCR LSC method) and the uncertainties related to the weighing of the samples.

For the case of ^{18}F , a solution with $1.5 \times 10^{-4} \text{ M}$ of BMIMHPTS in

Table 1

Theoretical and experimental ^{32}P and ^{18}F efficiencies for the logical sum of double coincidences, ε_D , for BMIMHPTS in BMIMCl. The theoretical efficiencies were calculated for both anisotropic ($\alpha = 0.42$) and isotropic ($\alpha = 1/3$) cases.

Cocktail	Concentration (mM)	TDCR	$\alpha = 0.42$	Experimental	$\alpha = 1/3$
^{18}F - Efficiency					
1	0	0.1186	0.0547	0.0563(9)	0.0493
2	0.015	0.1300	0.0630	0.0592(9)	0.0568
5	0.15	0.2198	0.1319	0.1264(19)	0.1206
8	1.5	0.1312	0.0639	0.0589(9)	0.0576
^{32}P - Efficiency					
1	0	0.5455	0.5734	0.5769(43)	0.5472
2	0.015	0.5941	0.6117	0.6064(45)	0.5862
3	0.035	0.6253	0.6351	0.6245(47)	0.6103
4	0.071	0.6384	0.6447	0.6317(47)	0.6202
5	0.14	0.6643	0.6633	0.6495(49)	0.6395
6	0.31	0.6777	0.6727	0.6576(49)	0.6494
7	0.72	0.6688	0.6665	0.6514(49)	0.6498
8	1.4	0.6397	0.6456	0.6324(47)	0.6212

BMIMCl yields a maximum ε_D value of $\sim 13\%$, more than twice the value obtained in pure BMIMCl. For ^{32}P , a concentration of $3 \times 10^{-4} \text{ M}$ of BMIMHPTS yields a maximum ε_D value of $\sim 66\%$, showing an increase of almost 14% compared with pure BMIMCl. As expected, the relative increase of the efficiencies is less when the efficiency value is higher, which is a direct consequence of the exponential relationship between the mean number of photons detected and the detection probability (see Eq. (1)). This improvement is particularly useful for detecting electron emissions with low energies close to the threshold energy.

A control experiment with ^{14}C does not show coincidence events above the background, rejecting another kind of luminescence that could eventually cause coincidences in the photomultiplier tubes.

The differences in the experimental optimal concentrations obtained for ^{18}F and ^{32}P can be assigned, in principle, to the different gaps between consecutive concentrations used for each radionuclide. Further measurements will be needed to elucidate if the optimal concentrations are, in fact, different.

The ε_D values found in this work are significantly lower than those reported by Kossert (2010) and Kossert et al. (2014). There are several factors (e.g., geometry and material of the optical chamber, kind of vials, photocathode sensitivity) that can strongly affect the overall efficiency of the TDCR system. Nonetheless, measurements performed with BMIMCl as solvent will get higher efficiencies than those performed with the same radionuclide in 1 M of HCl (in the same TDCR system). In our case, experimental ε_D values for ^{32}P , at the optimal concentration of the wavelength shifter, are $\sim 32\%$ higher than the ones obtained using a 1 M HCl aqueous solution ($\varepsilon_D \sim 50\%$).

Fig. 5 shows the experimental and the theoretical ε_D values as a function of BMIMHPTS concentration for both ^{18}F and ^{32}P radionuclides. The dashed line corresponds to $\alpha = 0.42$ (anisotropic luminescence), while the dotted line corresponds to $\alpha = 1/3$ (isotropic luminescence).

It is interesting to note that the experimental ε_D values approach the theoretical isotropic value ($\alpha = 1/3$) as the concentration increases. This trend is in agreement with the expected wavelength shift effect on the original anisotropic nature of the Čerenkov radiation since its fluorescence emission has to be isotropic. In this way, the addition of BMIMHPTS not only increases ε_D values but also breaks the anisotropy of the original Čerenkov emission.

4. Conclusions and perspectives

The wavelength shift effect of a highly fluorescent IL on the Čerenkov radiation originated from BMIMCl was studied. We showed that the luminescence Čerenkov spectra of pure BMIMCl shifts to higher

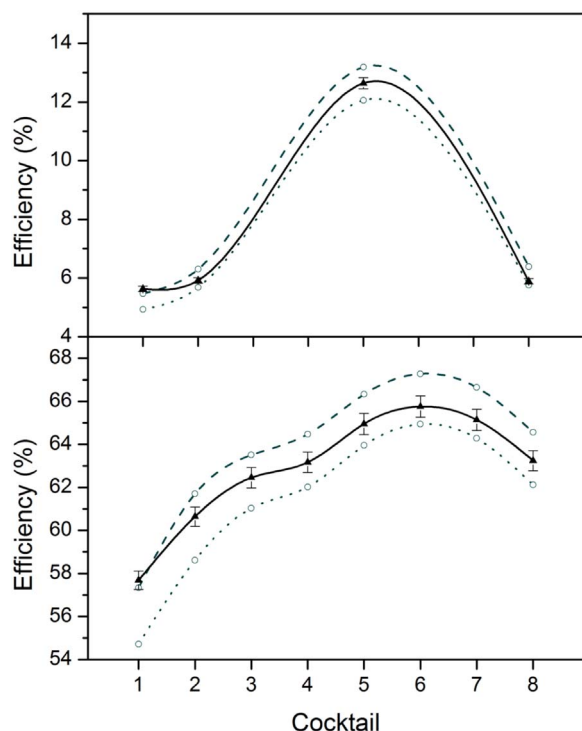


Fig. 5. Detection efficiencies for the logical sum of double coincidences, ϵ_D , calculated by TDCR-Čerenkov method for different concentrations of BMIMHPTS in BMIMCl, for ^{18}F (upper panel) and ^{32}P (lower panel). Dashed line corresponds to anisotropic case ($\alpha = 0.42$), dotted line corresponds to isotropic case ($\alpha = 1/3$), and solid line to the experimental values.

wavelengths due to the addition of BMIMHPTS. For BMIMHPTS concentration of the order of 10^{-4} M, both ^{18}F and ^{32}P detection efficiencies are increased around 124% and 14% compared with pure BMIMCl, respectively. Considering the low concentration values for which the maximum ϵ_D value is reached, a radiative transfer appears as the more suitable mechanism to explain this behavior. Furthermore, through the study of the effect of the α parameter, we verify that the addition of the wavelength shifter breaks the anisotropic nature of the Čerenkov radiation.

The improvement presented here is particularly useful for detecting electron emissions with energies close to the threshold energy. Clearly, despite the improvement in the achieved efficiencies, this method cannot replace liquid scintillation counting (LSC) and that is not the intention. Nevertheless, ILs offer some stimulating features: compared with other solvents with similar refraction index our IL mixture can be reused -when working with short-lived radionuclides- by simply

removing all water content in a vacuum oven. In addition, the ionic nature of ILs prevents the loss of material by evaporation, avoiding environmental pollution.

Acknowledgements

Funding was obtained from ANPCyT (PICT 2011–2378) and CONICET (PIP 11220130100795CO). M.M. is a staff member of CONICET and CNEA. D.R. has a post-doctoral fellowship from CONICET. G.P.S. has a post-doctoral fellowship from CNEA. Authors would like to express special thanks to: Marianela Lobos, Gabriela Cerruti y María Clara Ferrari for kindly support for sample preparations; Enrique San Roman for providing the cut-off filters; and Hugo Bianchi for providing optical elements.

References

- Arenillas, P., Cassette, P., 2006. Implementation of the TDCR liquid scintillation method at CNEA-LMR, Argentina. *Appl. Radiat. Isot.* 64, 1500–1504.
- Bé, M., Chisté, M., Dulieu, V., Browne, C., Chechev, E., Kuzmenko, V., N., Helmer, R., Nichols, A., Schönfeld, E., Dersch, R., 2004. Table of Radionuclides. Monographie BIPM-5.
- Dawson, W.R., Windsor, M.W., 1968. Fluorescence yields of aromatic compounds. *J. Phys. Chem.* 72, 3251–3260.
- ESTAR, 2009. <<http://physics.nist.gov/PhysRefData/Star/Text/ESTAR.html>>.
- Frank, I.M., Tamm, I.G., 1937. Coherent visible radiation of fast electrons passing through matter. *Compt. Rend. Acad. Sci. URSS* 14, 109–114.
- Förster, T., 1950. Die pH-Abhängigkeit der Fluoreszenz von Naphthalinderivaten. *Z. Elektrochem.* 54, 42–53.
- Isik, M., Sardon, H., Mecerreyes, D., 2014. Ionic liquids and cellulose: dissolution, chemical modification and preparation of new cellulosic materials. *Int. J. Mol. Sci.* 15, 11922–11940.
- Krimer, N., Rodrigues, D., Rodríguez, H., Mirenda, M., 2016. Steady-state fluorescence of highly absorbing samples in transmission geometry: a simplified quantitative approach considering re-absorption events. *Anal. Chem.* 89, 640–647.
- Kossert, K., 2010. Activity standardization by means of a new TDCR-Čerenkov counting technique. *Appl. Radiat. Isot.* 68, 1116–1120.
- Kossert, K., Grau Carles, A., Nähle, O., J., 2014. Improved Čerenkov counting techniques based on a free parameter model. *Appl. Radiat. Isot.* 86, 7–12.
- Mirenda, M., Rodrigues, D., Arenillas, P., Gutkowski, K., 2014. Ionic liquids as solvents for liquid scintillation technology. Čerenkov counting with 1-butyl-3-methylimidazolium chloride. *Rad. Phys. Chem.* 98, 98–102.
- Sarmiento, G.P., Zelcer, A., Espinosa, M.S., Babay, P.A., Mirenda, M., 2016. Photochemistry of imidazolium cations. Water addition to methylimidazolium ring induced by UV radiation in aqueous solution. *J. Photochem. Photobiol. A: Chem.* 314, 155–163.
- Sun, X., Luo, H., Dai, S., 2012. Ionic liquids-based extraction: a promising strategy for the advanced nuclear fuel cycle. *Chem. Rev.* 112, 2100–2128.
- Tamm, I., 1939. Radiation emitted by uniformly moving electrons. *J. Phys.* 1, 439–454.
- Turro, N.J., 1991. *Modern Molecular Photochemistry*. University Science Books, Sausalito, USA, pp. 318.
- Weingärtner, H., 2008. Understanding ionic liquids at the molecular level: facts, problems, and controversies. *Angew. Chem. Int. Ed. Engl.* 47, 654–670.
- Welton, T., 1999. Room-temperature ionic liquids. solvents for synthesis and catalysis. *Chem. Rev.* 99, 2071–2084.